Theoretical and Applied Fracture Mechanics 52 (2009) 183–194

Contents lists available at ScienceDirect

Theoretical and Applied Fracture Mechanics

journal homepage: www.elsevier.com/locate/tafmec

A review of the volume-based strain energy density approach applied to V-notches and welded structures

F. Berto *, P. Lazzarin

University of Padova, Department of Management and Engineering, Stradella San Nicola 3, Vicenza 36100, Italy

ARTICLE INFO

Article history:
Available online 8 October 2009

Keywords:
Strain energy density
Control radius
Finite-size volume
U-notch
V-notch
Welded joints

ABSTRACT

A large bulk of experimental data from static tests of sharp and blunt V-notches and from fatigue tests of welded joints are presented in an unified way by using the mean value of the Strain Energy Density (SED) over a given finite-size volume surrounding the highly stressed regions. When the notch is blunt, the control area assumes a crescent shape and R_0 is its width as measured along the notch bisector line. In plane problems, when cracks or pointed V-notches are considered, the volume becomes a circle or a circular sector, respectively. The radius R_0 depends on material fracture toughness, ultimate tensile strength and Poisson's ratio in the case of static loads; it depends on the fatigue strength $\Delta\sigma_A$ of the butt ground welded joints and the Notch Stress Intensity Factor (NSIF) range ΔK_1 in the case of welded joints under high cycle fatigue loading (with $\Delta\sigma_A$ and ΔK_1 valid for 5×10^6 cycles).

Dealing with welded joints characterised by a plate thickness greater than 6 mm, the final synthesis based on SED summarises nine hundred data taken from the literature while a new synthesis from spot-welded joints under tension and shear loading, characterised by a limited thickness of the main plate, is presented here for the first time (more than two hundred data).

Dealing with static tests, about one thousand experimental data as taken from the recent literature are involved in the synthesis. The strong variability of the non-dimensional radius R/R_0, ranging from about zero to about 1000, makes the check of the approach based on the mean value of the SED severe.

1. Introduction

Dealing with fracture assessment of cracked and notched components a clear distinction should be done between large and small bodies [1–6]. The design rules applied to large bodies are based on the idea that local inhomogeneities, where material damage starts, can be averaged being large the volume to surface ratio. In small bodies the high ratio between surface and volume makes not negligible the local discontinuities present in the material and the adoption of a multiscaling and segmentation scheme is the only way to capture what happens at pico-, nano- and micro-levels [4–6]. In this scheme the crack tip has no dimension or mass to speak; it is the sink and source that absorbs and dissipates energy while the stress singularity representation at every level is the most powerful tool to quantify the energy packed by an equivalent crack reflecting both material effect and boundary conditions. This new revolutionary representation implies also a new definition of mass [4,6]. The distinction between large and small bodies should ever be considered by avoiding to transfer directly the design rules valid for large components to small ones under the hypothesis that all material inhomogeneities can be averaged [1–6].

Keeping in mind the observations above and limiting our considerations to large bodies (i.e. large volume to surface ratio), for which an averaging process is still valid, the paper is addressed to review a volume-based Strain Energy Density Approach applied to Static and Fatigue Strength assessments of notched and welded structures [7–14].

The concept of "elementary" volume and "structural support length" was introduced many years ago [15–17] and it states that not the theoretical maximum notch stress is the static or fatigue strength-effective parameter in the case of pointed or sharp notches, but rather the notch stress averaged over a short distance normal to the notch edge. In high cycle fatigue regime, the integration path should coincide with the early fatigue crack propagation path. A further idea was to determine the fatigue-effective notch stress directly (i.e. without notch stress averaging) by performing the notch stress analysis with a fictitiously enlarged notch radius, ρ_f, corresponding to the relevant support [15–17].

Fundamentals of Critical Distance Mechanics applied to static failure, state that crack propagation occurs when the normal strain [18] or circumferential stress $\sigma_{\theta\theta}$ [19] at some critical distance from the crack tip reaches a given critical value. This "Point

* Corresponding author.
E-mail address: berto@gest.unipd.it (F. Berto).

0167-8442/$ - see front matter © 2009 Elsevier Ltd. All rights reserved.
doi:10.1016/j.tafmec.2009.10.001

Criterion" becomes a "Line criterion" in [20,21]. A stress criterion of brittle failure was proposed based on the assumption that crack initiation or propagation occurs when the mean value of decohesive stress over a specified damage segment d_0 reaches a critical value. The length d_0 is 2–5 times the grain size and then ranges for most metals from 0.03 mm to 0.50 mm. The segment d_0 was called "elementary increment of the crack length". Dealing with this topic a previous paper, [22], was quoted in [20,21]. Afterwards, this critical distance-based criterion was extended also to structural elements under multi-axial loading [23,24] by introducing a non-local failure function combining normal and shear stress components, both normalised with respect to the relevant fracture stresses of the material. Dealing with notched components the idea that a quantity averaged over a finite-size volume controls the stress state in the volume by means of a single parameter, the average circumferential $\sigma_{\theta\theta}$ stress, was suggested in [25].

For many years the Strain Energy Density (SED) has been used to formulate failure criteria for materials exhibiting both ductile and brittle behavior. As early as the work of [26], the SED has been found as a powerful tool to assess the static and fatigue behavior of notched and unnotched components in structural engineering. Different SED-based approaches were formulated by many researchers.

Dealing here with the strain energy density concept, it is worthwhile contemplating some fundamental contributions [27–35]. The concept of "core region" surrounding the crack tip was proposed in [27]. The main idea is that the continuum mechanics stops short at a distance from the crack tip, providing the concept of the radius of the core region. The strain energy density factor S was defined as the product of the strain energy density by a critical distance from the point of singularity [28]. Failure was thought of as controlled by a critical value S_c, whereas the direction of crack propagation was determined by imposing a minimum condition on S. The theory was extended to employ the total strain energy density near the notch tip [29], and the point of reference was chosen to be the location on the surface of the notch where the maximum tangential stress occurs. The strain energy density fracture criterion was refined and extensively summarised in Ref. [30]. The material element is always kept at a finite distance from the crack or the notch tip outside the "core region" where the inhomogeneity of the material due to micro-cracks, dislocations and grain boundaries precludes an accurate analytical solution. The theory can account for yielding and fracture and is applicable also to ductile materials. Depending on the local stress state, the radius of the core region may or may not coincide with the critical ligament r_c that corresponds to the onset of unstable crack extension [30]. The ligament r_c depends on the fracture toughness K_{Ic}, the yield stress σ_y, the Poisson's ratio v and, finally, on the ratio between dilatational and distortional components of the strain energy density. The direction of σ_{max} determines maximum distortion while σ_{min} relates to dilatation. Distortion is associated with yielding, dilatation tends to be associated to the creation of free surfaces or fracture and occurs along the line of expected crack extension [30,31].

A critical value of strain energy density function $(dW/dV)_c$ has been extensively used since 1965 [32–35], when first the ratio $(dW/dV)_c$ was determined experimentally for various engineering materials by using plain and notched specimens. The deformation energy required for crack initiation in a unit volume of material is called Absorbed Specific Fracture Energy (ASFE) and its links with the critical value of J_c and the critical factor S_c were widely discussed. This topic was deeply considered in [28–30] where it was showed that $(dW/dV)_c$ is equivalent to S_c/r being S_c the critical strain energy density factor and the radius vector r the location of failure. Since distributions of the absorbed specific energy W in notched specimens are not uniform, it was assumed that the specimen cracks as soon as a precise energy amount has been absorbed by the small plastic zone at the root of the notch. If the notch is sufficiently sharp, specific energy due to the elastic deformation is small enough to be neglected as an initial approximation [34]. While measurements of the energy in an infinitely small element are not possible, they can be approximated with sufficient accuracy by calculating the fracture energy over the entire fractured cross section of an unnotched tensile specimen [35]. Notched components loaded under static loads show that the average ASFE decreases with increasing the notch sharpness, with the ASFE parameter being plotted as a function of the theoretical stress concentration factor, K_t, and the temperature [35]. For a common welded structural steel and $K_t = 1$, the ASFE value, obtained by tensile tests, is about 1.0 MJ/m^3 while for values of K_t greater than 3.0 a plateau value is visible [35]. Depending on the considered welded metal, the plateau approximately ranges between 0.15 and 0.35 MJ/m^3. These values are not so different from the mean value that characterises the high cycle fatigue strength of welded joints, $W_c = 0.105$ MJ/m^3 but with reference to a specific control volume [8,10].

The criterion based on the energy density factor, S, gave a sound theoretical basis to the experimental findings [32–35] and the approach, used in different fields, was strongly supported by a number of researchers [36]. Recently as stated above, the volume energy function has been scaled from macro to micro to take into account the micro-cracks with a stronger stress singularity [2]. Dealing with pointed V-notches the volume energy density factor S was defined and applied as an extension of the method proposed for the crack case [31]. Potential sites of fracture initiation were assessed and the rate change of volume with surface $\Delta V/\Delta A$ was accurately evaluated by using numerical models showing that the local variation of this parameter should be kept smaller than the global average of $\Delta V/\Delta A$ in the system to assure the reliability of the numerical results. Moreover the critical strain energy density factor, S_c, was plotted as a function of the notch opening angle both for symmetrical and skew-symmetrical loadings. The fundamental hypothesis was that the location of yield and fracture initiation would coincide with the maximum of the maximum strain energy density function, $(dW/dV)^{max}_{max}$, and maximum of the minimum strain energy density function, $(dW/dV)^{max}_{min}$, with reference to the angular space variable, respectively. The stationary values of dW/dV in a system may have numerous maxima and minima. The pair $(dW/dV)^{max}_{max}$ and $(dW/dV)^{max}_{min}$ is unique and corresponds to a specific physical meaning. The peak of $(dW/dV)_{max}$, corresponding to a relative maximum, refers to yield because shape alteration with small volume change while the relative minimum corresponding to an increasing volume change is related to fracture. The second hypothesis is that failure by yielding and fracture would occur when $(dW/dV)^{max}_{max}$ and $(dW/dV)^{max}_{min}$ reach their respective critical values, $(dW/dV)_p$ and $(dW/dV)_c$.

The concept of strain energy density has also been reported in the literature in order to predict the fatigue behavior of notches both under uniaxial and multi-axial stresses [37,38].

It should be remembered that in referring to small-scale yielding, a method based on the averaged of the stress and strain product within the elastic–plastic domain around the notch was extended to cyclic loading of notched components [39]. In particular in [40] it was proposed a *fatigue master life curve* based on the use of the plastic strain energy per cycle as evaluated from the cyclic *hysteresis loop* and the positive part of the elastic strain energy density. The two views, cyclic hysteresis loop concept evaluating the plastic energy for tensile specimens [39,40] and the criterion evaluating the local accumulated SED near the crack tip [28], although formally different, are strictly connected and both tied to the concept of Absorbed Specific Fracture Energy.

The averaged strain energy density criterion, proposed in [7–14,41], states that brittle failure occurs when the mean value of

the strain energy density over a control volume (which becomes an area in two dimensional cases) is equal to a critical energy W_c. The SED approach is based both on a precise definition of the control volume and the fact that the critical energy does not depend on the notch sharpness. Such a method was formalised and applied first to sharp, zero radius, V-notches and later extended to blunt U- and V-notches under mode I loading [11] and successfully applied to welded joints [10]. The control radius R_0 of the volume, over which the energy has to be averaged, depends on the ultimate tensile strength, the fracture toughness and Poisson's ratio in the case of static loads, whereas it depends on the unnotched specimen's fatigue limit, the threshold stress intensity factor range and the Poisson's ratio under high cycle fatigue loads. The approach was successfully used under both static and fatigue loading conditions to assess the strength of notched and welded structures subjected to predominant mode I and also to mixed-mode loading [7–14]. The extension of the SED approach to ductile fracture is possible, with a major problem being the definition of the control volume and the influence of the dilatational and distortional components of the strain energy density. Recently, the effect of plasticity in terms of strain energy density over a given control volume has been considered by the present authors, showing different behaviours under tension and torsion loading, as well as under small and large scale yielding [14].

Several criteria have been proposed to predict fracture loads of components with *notches*, subjected to *mode I loading* [20,21,42–53]. Recently, fracture loads of notched specimens (sharp and blunted U- and V-notches) loaded under mode I have been successfully predicted, using a criterion based on the cohesive zone model [54–57], and in parallel by applying the local strain energy density [7–14]. The problem of brittle failure from *blunted notches* loaded under *mixed mode* is more complex than in mode I loading and experimental data, particularly for notches with a non-negligible radius, is scarce. The main aim of some recent papers was to generalise the previous results valid for components with blunted notches loaded under mode I, to notched components loaded under mixed mode [58–61]. This generalization is based on the hypothesis that fracture mainly depends on the local mode I and on the maximum value of the principal stress or the strain energy density. The proposal of mode I dominance for cracked plates was suggested first in [62] when dealing with cracked plates under plane loading and transverse shear, where the crack grows in the direction almost perpendicular to the maximum tangential stress in radial direction from its tip. Two different methods are used to verify such a hypothesis: the cohesive zone model and the model based on the strain energy density over a control volume [58–60]. Both methods allow to evaluate the critical load under different mixed-mode conditions when the material behaviour can be assumed as linear elastic. Dealing with the SED approach it is worth noting that the case of pure compression or combined compression and shear, for example, would require a reformulation for the control radius of the volume, R_0, and should also take into account the variability of the critical strain energy density W_c with respect to the case of uniaxial tension loads. To the best of authors' knowledge, the first contribution that modifies the total strain energy density criterion (Beltrami hypothesys) to account for the different strength properties exhibited by many materials under pure tension and pure compression uniaxial tests was dated 1926 [63].

Dealing with both notched and welded components and summarising the most recent experimental results reported in the literature, the main aim of the present contribution is to present a complete review of the analytical frame of the volume-based SED approach together with a final synthesis of more than 1900 experimental data from static and fatigue tests. Very different materials have been considered with a control radius, R_0, ranging from 0.4 to 500 μm.

2. Some expressions for SED in the control volume

With the aim of clarifying the base of the final synthesis carried out in this paper, this section summarises the analytical frame of SED approach.

2.1. Stress distributions due to U- and V-notches

With reference to the polar coordinate system shown in Fig. 1, with the origin located at point O, mode I stress distribution ahead of a V-notch tip is given by the following expressions [64]:

$$\sigma_{ij} = a_1 r^{\lambda_1 - 1}\left[f_{ij}(\theta,\alpha) + \left(\frac{r}{r_0}\right)^{\mu_1-\lambda_1} g_{ij}(\theta,\alpha)\right] \tag{1}$$

where $\lambda_1 > \mu_1$ and the parameter a_1 can be expressed either via the notch stress intensity factor K_1 in the case of a sharp, zero radius, V-notch or by means of the elastic maximum notch stress σ_{tip} in the case of blunt V-notches. In Eq. (1), r_0 is the distance evaluated on the notch bisector line between the V-notch tip and the origin of the local coordinate system; r_0 depends both on the notch root radius R and the opening angle 2α (Fig. 2), according to the expression $r_0 = R[(\pi - 2\alpha)/(2\pi - 2\alpha)]$. The angular functions f_{ij} and g_{ij} are given in [64]:

$$\begin{Bmatrix} f_{\theta\theta} \\ f_{rr} \\ f_{r\theta} \end{Bmatrix} = \frac{1}{1+\lambda_1+\chi_{b_1}(1-\lambda_1)}\left[\begin{Bmatrix} (1+\lambda_1)\cos(1-\lambda_1)\theta \\ (3-\lambda_1)\cos(1-\lambda_1)\theta \\ (1-\lambda_1)\sin(1-\lambda_1)\theta \end{Bmatrix} + \chi_{b_1}(1-\lambda_1)\begin{Bmatrix} \cos(1+\lambda_1)\theta \\ -\cos(1+\lambda_1)\theta \\ \sin(1+\lambda_1)\theta \end{Bmatrix}\right] \tag{2}$$

$$\begin{Bmatrix} g_{\theta\theta} \\ g_{rr} \\ g_{r\theta} \end{Bmatrix} = \frac{q}{4(q-1)[1+\lambda_1+\chi_{b_1}(1-\lambda_1)]}\left(\chi_{d_1}\begin{Bmatrix} (1+\mu_1)\cos(1-\mu_1)\theta \\ (3-\mu_1)\cos(1-\mu_1)\theta \\ (1-\mu_1)\sin(1-\mu_1)\theta \end{Bmatrix} + \chi_{c_1}\begin{Bmatrix} \cos(1+\mu_1)\theta \\ -\cos(1+\mu_1)\theta \\ \sin(1+\mu_1)\theta \end{Bmatrix}\right) \tag{3}$$

The eigenfunctions f_{ij} depend only on Williams' eigenvalue, λ_1, which controls the sharp solution for zero notch radius [65]. The eigenfunctions g_{ij} mainly depend on eigenvalue μ_1, but are not independent from λ_1. Since $\mu_1 < \lambda_1$, the contribution of μ-based terms in Eq. (1) rapidly decreases with the increase of the distance from the notch tip. All parameters in Eqs. (2) and (3) have closed-form expressions but here, for the sake of brevity, only some values for the most common angles are reported in Table 1 [64].

Under the plane strain conditions, the eigenfunctions f_{ij} and g_{ij} satisfy the following expressions:

$$f_{zz}(\theta) = \nu(f_{\theta\theta}(\theta) + f_{rr}(\theta)), \quad g_{zz}(\theta) = \nu(g_{\theta\theta}(\theta) + g_{rr}(\theta)) \tag{4}$$

whereas $f_{zz}(\theta) = g_{zz}(\theta) = 0$ under plane stress conditions.

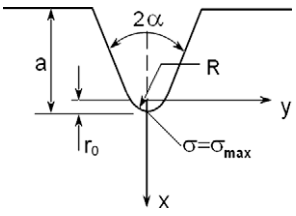

Fig. 1. Notch geometry and coordinate system.

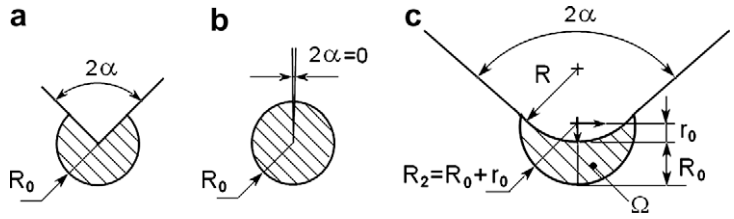

Fig. 2. Critical volume (area) for sharp V-notch (a), crack (b) and blunt V-notch (c) under mode I loading. Distance $r_0 = R \times (\pi - 2\alpha)/(2\pi - 2\alpha)$.

Table 1
Parameters for stress distributions and local strain energy [64].

2α [rad]	q	λ_1	μ_1	χ_{b1}	χ_{c1}	χ_{d1}	$\widetilde{\omega}_1$ $F(2\alpha)$	
0	2.0000	0.5	−0.5	1	4	0	1	0.7850
$\pi/6$	1.8333	0.5014	−0.4561	1.0707	3.7907	0.0632	1.034	0.6917
$\pi/4$	1.7500	0.5050	−0.4319	1.1656	3.5721	0.0828	1.014	0.6692
$\pi/3$	1.6667	0.5122	−0.4057	1.3123	3.2832	0.0960	0.970	0.6620
$\pi/2$	1.5000	0.5448	−0.3449	1.8414	2.5057	0.1046	0.810	0.7049
$2\pi/3$	1.3334	0.6157	−0.2678	3.0027	1.5150	0.0871	0.570	0.8779
$3\pi/4$	1.2500	0.6736	−0.2198	4.1530	0.9933	0.0673	0.432	1.0717
$5\pi/6$	1.1667	0.7520	−0.1624	6.3617	0.5137	0.0413	0.288	1.4417

2.2. Strain energy density approach

The SED approach is based on the idea that under tensile stresses failure occurs when $\overline{W} = W_c$, where the critical value W_c obviously varies from material to material. If the material behaviour is ideally brittle, then W_c can be evaluated by using simply the conventional ultimate tensile strength σ_t, so that $W_c = \sigma_t^2/2E$.

Often unnotched specimens exhibit a non-linear behaviour whereas the behaviour of notched specimens remains linear. Under these circumstances the stress σ_t should be substituted by "*the maximum normal stress existing at the edge at the moment preceding the cracking*", as underlined in [21] where it is also recommended to use tensile specimens with semicircular notches.

In plane problems, the control volume becomes a circle or a circular sector with a radius R_0 in the case of cracks or pointed V-notches in mode I or mixed, I + II, mode loading (Fig. 2a and b). Under plane strain conditions, a useful expression for R_0 has been provided considering the crack case [41]:

$$R_0 = \frac{(1+\nu)(5-8\nu)}{4\pi}\left(\frac{K_{IC}}{\sigma_t}\right)^2 \tag{5}$$

If the critical value of the NSIF is determined by means of specimens with $2\alpha \neq 0$, the critical radius can be estimated by means of the expression:

$$R_0 = \left[\frac{I_1 \times K_{1C}^2}{4\lambda_1(\pi-\alpha)EW_c}\right]^{1/(2-2\lambda_1)} \tag{6}$$

When $2\alpha = 0$, K_{1C} equals the fracture toughness K_{IC}.

In the case of blunt notches, the area assumes a crescent shape, with R_0 being its maximum width as measured along the notch bisector line (Fig. 2c) [11]. Under mixed-mode loading, the control area is no longer centred with respect to the notch bisector, but rigidly rotated with respect to it and centred on the point where the maximum principal stress reaches its maximum value [58,59]. This rotation is shown in Fig. 3 where the control area is drawn for a U-shaped notch both under mode I loading (Fig. 3a) and mixed-mode loading (Fig. 3b).

The parameter a_1 of Eq. (1) can be linked to the mode I notch stress intensity factor by means of the simple expression

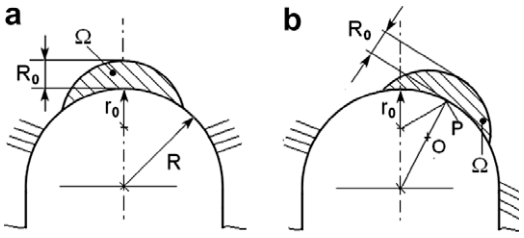

Fig. 3. Critical volume for U-notch under mode I (a) and mixed-mode loading (b). Distance $r_0 = R/2$ according to [15] and [66].

$$a_1 = \frac{K_1}{\sqrt{2\pi}} \tag{7}$$

where K_1 assumes the following form according to the definition given in Ref. [67]

$$K_1 = \sqrt{2\pi}\lim_{r\to 0}[\sigma_\theta(r,\theta=0)]r^{1-\lambda_1} \tag{8}$$

In the presence of a notch root radius equal to zero, the distance r_0 is also zero, and all μ-related terms in Eq. (1) disappear. It is possible to determine the total strain energy over the area of radius R_0 and then the mean value of the elastic SED referred to the area Ω. The final relationship is

$$\overline{W}_1 = \frac{I_1}{4E\lambda_1(\pi-\alpha)}\left(\frac{K_1}{R_0^{1-\lambda_1}}\right)^2 \tag{9}$$

where λ_1 is Williams' eigenvalue and K_1 the mode I notch stress intensity factor. The parameter I_1 is different under plane stress and plane strain conditions and is given in Table 2 for different values of the Poisson's ratio ν [60]. Eq. (9) was extended to pointed V-notches in mixed, I + II, mode [7] as well as to cases where mode I loads where combined with mode III loads [9]. While describing Table 2 it is important to underline the influence of the Poisson's ratio on the I_1 values in the case of sharp notches. For a notch opening angle smaller than 60°, I_1 varies strongly from $\nu = 0.1$ to $\nu = 0.4$. This fact confirms the important and not negligible effect of the Poisson's ratio while discussing sharp or quasi-sharp notches in agreement with the effect of this parameter on the kind of singularities, weak or strong, highlighted in [1] in the case of a constrained micro-notch at the front of a free edge macro-crack.

Table 2
Parameter I_1 for sharp, zero radius, V-notches (plane strain) [7,60].

2α (°)	γ/π (rad)	λ_1	I_1						
			$\nu = 0.10$	$\nu = 0.15$	$\nu = 0.2$	$\nu = 0.25$	$\nu = 0.3$	$\nu = 0.35$	$\nu = 0.4$
0	1	0.5000	1.1550	1.0925	1.0200	0.9375	0.8450	0.7425	0.6300
15	23/24	0.5002	1.1497	1.0880	1.0162	0.9346	0.8431	0.7416	0.6303
30	11/12	0.5014	1.1335	1.0738	1.0044	0.9254	0.8366	0.7382	0.6301
45	7/8	0.5050	1.1063	1.0499	0.9841	0.9090	0.8247	0.7311	0.6282
60	5/6	0.5122	1.0678	1.0156	0.9547	0.8850	0.8066	0.7194	0.6235
90	3/4	0.5445	0.9582	0.9173	0.8690	0.8134	0.7504	0.6801	0.6024
120	2/3	0.6157	0.8137	0.7859	0.7524	0.7134	0.6687	0.6184	0.5624
135	5/8	0.6736	0.7343	0.7129	0.6867	0.6558	0.6201	0.5796	0.5344
150	7/12	0.7520	0.6536	0.6380	0.6186	0.5952	0.5678	0.5366	0.5013

2.3. Strain energy density for blunt V-notches under mode I loading

In the presence of rounded V-notches it is possible to link the parameter a_1 of Eq. (1) to the maximum principal stress present at the notch tip:

$$a_1 = \frac{\sigma_{tip} r_0^{1-\lambda_1}}{1+\widetilde{\omega}_1} \tag{10}$$

where $\widetilde{\omega}_1$ is the parameter already listed in Table 1. By using the elastic maximum notch stress, it is possible to determine the total strain energy over the area Ω and then the mean value of the SED. When the area embraces the semicircular edge of the notch (and not its rectilinear flanks), the mean value of SED can be expressed in the following form [11]:

$$\overline{W}_1 = F(2\alpha) \times H\left(2\alpha, \frac{R_0}{R}\right) \times \frac{\sigma_{tip}^2}{E} \tag{11}$$

where $F(2\alpha)$ depend on previously defined parameters

$$F(2\alpha) = \left(\frac{q-1}{q}\right)^{2(1-\lambda_1)} \left[\frac{\sqrt{2\pi}}{1+\widetilde{\omega}_1}\right]^2 \tag{12}$$

and is reported in the last column of Table 1. H is summarised in Tables 3 and 4 as a function of opening angles and Poisson's ratios. By simply using the definition of the mode I NSIF for blunt V-notches [68] a simple relationship between σ_{tip} and $K_{R,I}^V$ can be obtained as follows:

Table 4
H values for U-notched specimens [11].

R_0/R	H				
	$\nu = 0.1$	$\nu = 0.15$	$\nu = 0.2$	$\nu = 0.25$	$\nu = 0.3$
0.0005	0.6294	0.6215	0.6104	0.5960	0.5785
0.001	0.6286	0.6207	0.6095	0.5952	0.5777
0.005	0.6225	0.6145	0.6033	0.5889	0.5714
0.01	0.6149	0.6068	0.5956	0.5813	0.5638
0.05	0.5599	0.5515	0.5401	0.5258	0.5086
0.1	0.5028	0.4942	0.4828	0.4687	0.4518
0.3	0.3528	0.3445	0.3341	0.3216	0.3069
0.5	0.2672	0.2599	0.2508	0.2401	0.2276
1	0.1590	0.1537	0.1473	0.1399	0.1314

$$K_{R,I}^V = \sqrt{2\pi}\frac{\sigma_{tip}}{1+\widetilde{\omega}_1}\left(\frac{q-1}{q}R\right)^{1-\lambda_1} = \sqrt{F(2\alpha)}\sigma_{tip}R^{1-\lambda_1} \tag{13}$$

Then it is possible to rewrite Eq. (11) in a more compact form:

$$\overline{W}_1 = H\left(2\alpha, \frac{R_0}{R}\right) \times \frac{(K_{R,I}^V)^2}{E} \times \frac{1}{R_0^{2(1-\lambda_1)}} \tag{14}$$

Eq. (14) will be used to summarise all results from blunt notches (U- and V-notches) subjected to mode I loading.

2.4. Strain energy density for blunt notches under mixed-mode loading

Under mixed-mode loading the problem becomes more complex than under mode I loading, mainly because the maximum elastic stress is out of the notch bisector line and its position varies

Table 3
Values of the function H for blunted V-shaped notches [11].

2α (rad)	R_0/R	H			2α (rad)	R_0/R	H		
		$\nu = 0.3$	$\nu = 0.35$	$\nu = 0.4$			$\nu = 0.3$	$\nu = 0.35$	$\nu = 0.4$
0	0.01	0.5638	0.5432	0.5194	$\pi/2$	0.01	0.6290	0.6063	0.5801
	0.05	0.5086	0.4884	0.4652		0.05	0.5627	0.5415	0.5172
	0.1	0.4518	0.4322	0.4099		0.1	0.4955	0.4759	0.4535
	0.3	0.3069	0.2902	0.2713		0.3	0.3296	0.3144	0.2972
	0.5	0.2276	0.2135	0.1976		0.5	0.2361	0.2246	0.2115
	1	0.1314	0.1217	0.1110		1	0.1328	0.1256	0.1174
$\pi/6$	0.01	0.6395	0.6162	0.5894	$2\pi/3$	0.01	0.5017	0.4836	0.4628
	0.05	0.5760	0.5537	0.5280		0.05	0.4465	0.4298	0.4106
	0.1	0.5107	0.4894	0.4651		0.1	0.3920	0.3767	0.3591
	0.3	0.3439	0.3264	0.3066		0.3	0.2578	0.2467	0.2339
	0.5	0.2531	0.2386	0.2223		0.5	0.1851	0.1769	0.1676
	1	0.1428	0.1333	0.1226		1	0.1135	0.1079	0.1015
$\pi/3$	0.01	0.6678	0.6436	0.6157	$3\pi/4$	0.01	0.4114	0.3966	0.3795
	0.05	0.5998	0.5769	0.5506		0.05	0.3652	0.3516	0.3359
	0.1	0.5302	0.5087	0.4842		0.1	0.3206	0.3082	0.2938
	0.3	0.3543	0.3372	0.3179		0.3	0.2082	0.1997	0.1900
	0.5	0.2597	0.2457	0.2301		0.5	0.1572	0.1504	0.1427
	1	0.1435	0.1349	0.1252		1	0.1037	0.0988	0.0932

as a function of mode I–II stress distributions (see Fig. 3). The problem was widely discussed considering different combination of mode mixity [58,59].

The expression for U-notches under mixed mode is analogous to that valid for notches in mode I:

$$\overline{W}^{(e)} = H^*\left(2\alpha, \frac{R_0}{R}\right) \times \frac{\pi\sigma_{max}^2}{4E} \tag{15}$$

where σ_{max} is the maximum value of the principal stress along the notch edge and H^* depends again on the normalised radius R/R_0, the Poisson's ratio ν and the loading conditions. For different configurations of mode mixity, the function H, analytically obtained under mode I loading, was shown to be very close to H^*. This idea of equivalent local mode I was discussed in previous works [58,59]. Eq. (15) will be used here to summarise all experimental data from U-notches under mixed-mode conditions. When the notch opening angle is different from zero, the SED should be directly evaluated from FE models being $\lambda_1 \neq \lambda_2$ in that case.

In order to better justify the choice of the control area Ω, consider Fig. 4 where a number of curves with different strain energy density values are plotted for a U-shaped notch ($2\alpha = 0$). The centre of the curved lines, as obtained from a FE analysis, is approximately located at a distance $r_0 = R/2$ with respect to the notch tip, that is in correspondence of the origin of the local coordinate system. An increase of the radius R_2, due to an increase of R_0, results in a reduction of the strain energy density level. Consider now a blunt V-notch with $2\alpha = 135°$ (Fig. 5). The centre of the strain energy density curves is seen to be much closer to the notch tip than in the previous case. A distance $r_0 = R/5$, in agreement with the theoretical model, seems to be a good approximation. An increase of R_2 (due to an increase of R_0, r_0 being constant) allows us to reach the curves with minor strain energy density. The greater R_0, the smaller the sensitivity to the notch is. When $R = 0$, the radius R_2 coincides with R_0 and becomes independent of the notch opening angle.

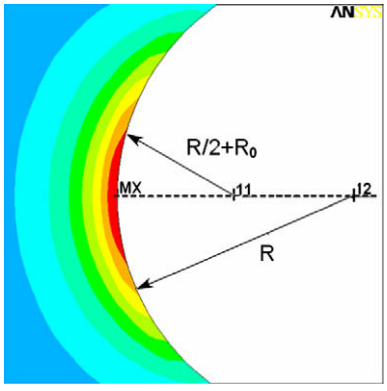

Fig. 4. Strain energy density curves for a U-shaped notch under mode I loading.

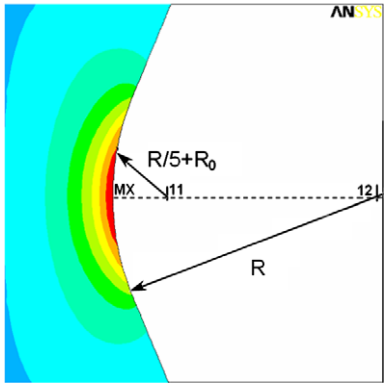

Fig. 5. Strain energy density curves for a V-shaped notch with $2\alpha = 135°$ under mode I loading.

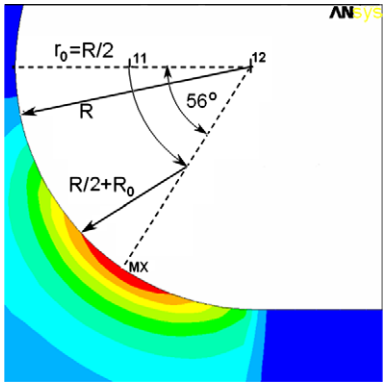

Fig. 6. Strain energy density curves for a U-shaped notch under shear loading.

In the presence of combined tension and shear loads, the point of the maximum principal stress does not coincide with the notch tip as stated above. The control volume moves as shown in Fig. 6: it rotates with respect to the centre of the notch root, according to an angle that depends on $K^V_{R,II}$ to $K^V_{R,I}$ ratio, where $K^V_{R,II}$ and $K^V_{R,I}$ are the mode II and mode I notch stress intensity factors for blunt U- and V-notches. However, in general, a major difficulty in applying the present approach to mixed-mode problems is the definition of the control volume, due to the differences between the critical value W_c under tension and compression tests exhibited by many materials. A possible strategy might be that of modifying Eq. (14) by adding an energetic term proportional to the mean stress, in order to take into account the sign of the stresses. The new expression should be compared with a critical value equal to $W^*_c = \beta\sigma_t^2/(2E)$, where β gives the compression strength to tensile strength ratio.

2.5. Some advantages of the SED

As opposed to the direct evaluation of the NSIFs, which needs very refined meshes, the mean value of the elastic SED on the control volume can be determined with high accuracy by using coarse meshes [69,70]. Very refined meshes are necessary to directly determined the NSIFs from the local stress distributions. Refined meshes are not necessary when the aim of the finite element analysis is to determine the mean value of the local strain energy density on a control volume surrounding the points of stress singularity. The SED in fact can be derived directly from nodal displacements, so that also coarse meshes are able to give sufficiently accurate values for it. Some recent contributions document the weak variability of the SED as determined from very refined meshes and coarse meshes, considering some typical welded joint geometries and provide a theoretical justification to the weak dependence exhibited by the mean value of the local SED when evaluated over a control volume centred at the weld root or the weld toe. On the contrary singular stress distributions are strongly mesh dependent. The NSIFs can be estimated from the local SED value of pointed V-notches in plates subjected to mode I, mode II or a mixed-mode loading. Taking advantage of some closed-form relationships linking the local stress distributions ahead of the notch to the maximum elastic stresses at the notch tip the coarse mesh SED-based procedure is used to estimate the relevant theoretical stress concentration factor K_t for blunt notches considering,

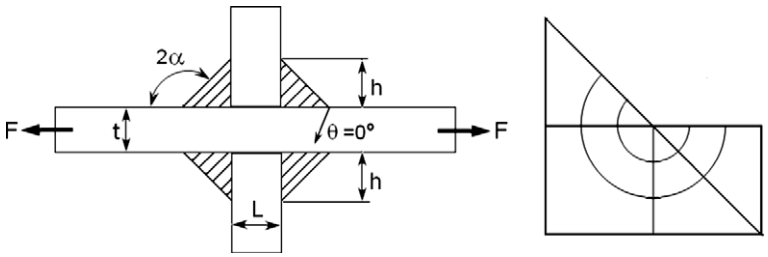

Fig. 7. Geometrical parameters for transverse non-load carrying fillet welded joints and modulus used at the weld toe for the SED evaluation.

in particular, a circular hole and a U-shaped notch, the former in mode I loading, the latter also in mixed, I + II, mode [69,70]. Fig. 7 shows for a particular geometry analysed in Ref. [69] the typical coarse mesh used to evaluate the SED at the weld toe. Inside the control volume eight elements were used and the entire model of the welded joint contained 40 elements being negligible the difference in terms of SED with the results obtained from finer meshes used for the NSIFs evaluation.

Other important advantages can be achieved by using the SED approach. The most important are as follows:

- It permits consideration of the scale effect which is fully included in the Notch Stress Intensity Factor Approach.
- It permits consideration of the contribution of different modes.
- It permits consideration of the cycle nominal load ratio.
- It overcomes the complex problem tied to the different NSIF units of measure in the case of different notch opening angles (i.e crack initiation at the toe ($2\alpha = 135°$) or root ($2\alpha = 0°$) in a welded joint).
- It overcomes the complex problem of multiple crack initiation and their interaction on different planes.
- It directly takes into account the *T*-stress and this aspect becomes fundamental when thin structures are analysed [71].
- It directly includes three-dimensional effects and out-of-plane singularities not assessed by Williams' theory [72–76].

3. Synthesis based on SED in a control volume

The mean value of the strain energy density (SED) in a circular sector of radius R_0 located at the fatigue crack initiation sites has been used to summarise fatigue strength data from steel welded joints of complex geometry.

Local strain energy density $\Delta\overline{W}$ averaged in a finite-size volume surrounding weld toes and roots is a scalar quantity which can be given as a function of mode I–II NSIFs in plane problems [8] and mode I–II–III NSIFs in three dimensional problems [9]. The evaluation of the local strain energy density needs precise information about the control volume size. From a theoretical point of view the material properties in the vicinity of the weld toes and the weld roots depend on a number of parameters as residual stresses and distortions, heterogeneous metallurgical micro-structures, weld thermal cycles, heat source characteristics, load histories and so on. To device a model capable of predicting R_0 and fatigue life of welded components on the basis of all these parameters is really a task too complex. Thus, the spirit of the approach is to give a simplified method able to summarise the fatigue life of components only on the basis of geometrical information, treating all the other effects only in statistical terms, with reference to a well-defined group of welded materials and, for the time being, to arc welding processes.

In a plane problem all stress and strain components in the highly stressed region are correlated to mode I and mode II NSIFs. Under a plane strain hypothesis, the strain energy included in a semicircular sector shown in Fig. 2 is [7,13]

$$\Delta\overline{W} = \left\{ \frac{e_1}{E}\left[\frac{\Delta K_1}{R_0^{1-\lambda_1}}\right]^2 + \frac{e_2}{E}\left[\frac{\Delta K_2}{R_0^{1-\lambda_2}}\right]^2 + \frac{e_3}{E}\left[\frac{\Delta K_3}{R_0^{1-\lambda_3}}\right]^2 \right\} \tag{16}$$

where R_0 is the radius of the semicircular sector and e_1, e_2 and e_3 are functions that depend on the opening angle 2α and the Poisson ratio ν (see Table 5).

The material parameter R_0 can be estimated by using the fatigue strength $\Delta\sigma_A$ of the butt ground welded joints (in order to quantify the influence of the welding process, in the absence of any stress concentration effect) and the NSIF-based fatigue strength of welded joints having a V-notch angle at the weld toe constant and large enough to ensure the non singularity of mode II stress distributions.

A convenient expression is [7]:

$$R_0 = \left(\frac{\sqrt{2e_1}\Delta K_{1A}}{\Delta\sigma_A}\right)^{\frac{1}{1-\lambda_1}} \tag{17}$$

where both λ_1 and e_1 depend on the V-notch angle. Eq. (17) makes it possible to estimate the R_0 value as soon as ΔK_{1A} and $\Delta\sigma_A$ are known. At $N_A = 5 \cdot 10^6$ cycles and in the presence of a nominal load ratio $\widetilde{R}$ equal to zero a mean value ΔK_{1A} equal to 211 MPa mm$^{0.326}$ was found re-analysing experimental results taking from the literature [10]. For butt ground welds made of ferritic steels a mean value $\Delta\sigma_A = 155$ MPa (at $N_A = 5 \cdot 10^6$ cycles, with $\widetilde{R} = 0$) was found [77].

Table 5
Values of the parameters in Eq. (16), valid for the Beltrami hypothesys and a Poisson's ratio $\nu = 0.3$.

2α (rad)	γ (rad)	λ_1	λ_2	λ_3	Plane strain		Axis-sym.
					e_1	e_2	e_3
0	π	0.5000	0.5000	0.5000	0.13449	0.34139	0.41380
$\pi/12$	$23\pi/24$	0.5002	0.5453	0.5217	0.13996	0.30588	0.39659
$\pi/6$	$11\pi/12$	0.5014	0.5982	0.5455	0.14485	0.27297	0.37929
$\pi/3$	$5\pi/6$	0.5122	0.7309	0.6000	0.15038	0.21530	0.34484
$\pi/2$	$3\pi/4$	0.5445	0.9085	0.6667	0.14623	0.16793	0.31034
$2\pi/3$	$2\pi/3$	0.6157	1.1489	0.7500	0.12964	0.12922	0.27587
$3\pi/4$	$5\pi/8$	0.6736	1.3021	0.8000	0.11721	0.11250	0.25863

Then, by introducing the above mentioned value into Eq. (17), one obtains for steel welded joints with failures from the weld toe $R_0 = 0.28$ mm.

It is interesting to learn that, for welded joints made of structural steels, different espressions for ΔK_{th} taken from the literature were reported in [78], from which $\Delta K_{th} = 180$ MPa mm$^{0.5}$ (5.7 MPa m$^{0.5}$). In the case $2\alpha = 0$ and fatigue crack initiation at the weld root Eq. (17) gives $R_0 = 0.36$ mm, by neglecting the mode II contribution and using $e_1 = 0.133$, Eq. (7), $\Delta K_{1A}^N = 180$ MPa mm$^{0.5}$, and, once again, $\Delta\sigma_A = 155$ MPa. This means that the choice to use a critical radius equal to 0.28 mm both for toe and root failures is a sound engineering approximation.

By modelling the weld toe regions as sharp V-notches and using the local strain energy, more than 300 fatigue strength data from welded joints with weld toe failure were analysed and the first theoretical scatter band in terms of SED was obtained [8]. The geometry exhibited a strong variability of the main plate thickness (from 6 to 100 mm), the transverse plate (from 3 to 200 mm) and the bead flank (from 110° to 150°). The synthesis of all those data is shown in Fig. 8, where the number of cycles to failure is given as a function of $\Delta\overline{W}_1$ (the mode II stress distribution being non singular for all those geometries). The figure includes data obtained both under tension and bending loads, as well as from "as-welded" and "stress-relieved" joints. The scatter index T_W, related to the two curves with probabilities of survival P_S= 2.3% and 97.7%, is 3.3, to be compared with the variation of the strain energy density range, from about 4.0 to about 0.1 MJ/m^3. $T_W = 3.3$ becomes equal to 1.50 when reconverted to an equivalent local stress range with probabilities of survival $P_S = 10\%$ and 90% ($T_\sigma = \sqrt{3.3}/1.21 = 1.5$). The scatter band proposed was latter applied in [10] to a larger bulk of experimental data, which included also fatigue failures from the weld root.

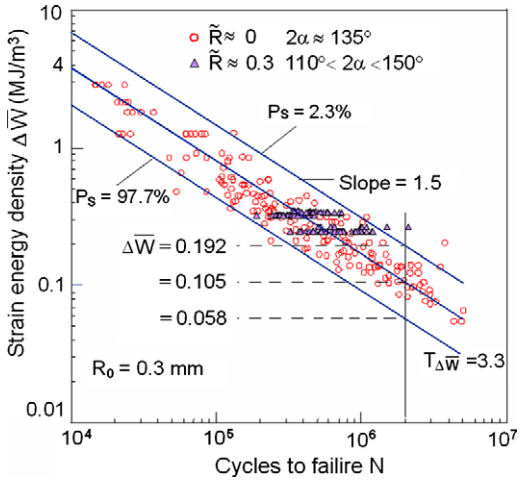

Fig. 8. Strain energy-based scatter band summarising more than 300 fatigue strength data from steel welded joints with weld toe failure. The main plate thickness ranged from 6 to 100 mm. $\tilde{R}$: nominal load ratio; 2α: V-notch angle at the weld toe [8].

A final synthesis based on 900 experimental data is shown in Fig. 9 where some recent results from butt welded joints, three-dimensional models and hollow section joints have been included. A good agreement is found, giving a sound, robust basis to the approach when the welded plate thickness is equal to or greater than 6 mm.

A new synthesis of data from single spot-welded joints (see Fig. 10) characterised by thin plates ($0.65\text{ mm} \leqslant t \leqslant 1.75$ mm) is presented here for the first time. The control radius of the three-dimensional volume around the slit tip and its depth are equal to 0.28 mm. The value of $\Delta\overline{W}$ at 2×10^6 cycles is higher than that reported in Fig. 9 and referred to main plate thicknesses greater than 6 mm ($\Delta\overline{W} = 0.18$ N mm/mm^3 for single spot-welded joints against $\Delta\overline{W} = 0.105$ N mm/mm^3 in Fig. 9). Future developments will be presented and widely discussed by the present authors in forthcoming publications.

Dealing with static loading, the local SED values are normalised to the critical SED values (as determined from unnotched specimens) and plotted as a function of the R/R_0 ratio. The data related to the experimental program of PMMA tested at −60 °C [56–59] are summarised together with other data taken from a data base related to PMMA tested at room temperature [45,54,55]. Dealing with cracked and V-sharp specimens under mixed mode I + II loading recent data taken from the literature are also considered in the present synthesis [79,80]. In particular data summarised in [79] are from sharp V-specimens made of an acrylic resin and tested under mixed-mode loading whereas in [80] data are from diagonally loaded square cracked plate specimens made of PMMA. Dealing with the acrylic resin, V-notched plates presented different opening angles (30°, 60° and 90°), and were also characterised by a notch axis differently inclined with respect to the minor side of the specimens (0°, 5°, 15° and 30°) [79]. The notch root radius was nominally equal to zero, whereas the R_0 was about equal to

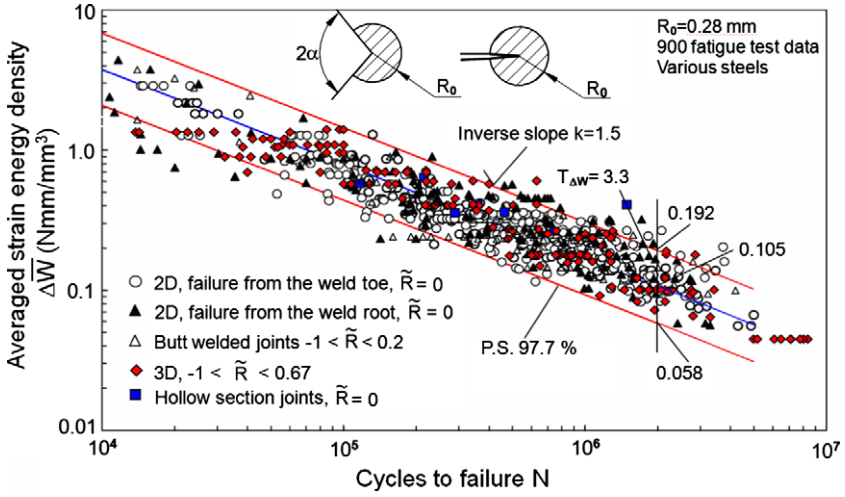

Fig. 9. Fatigue strength of welded joints as a function of the averaged local strain energy density; $\tilde{R}$ is the nominal load ratio.

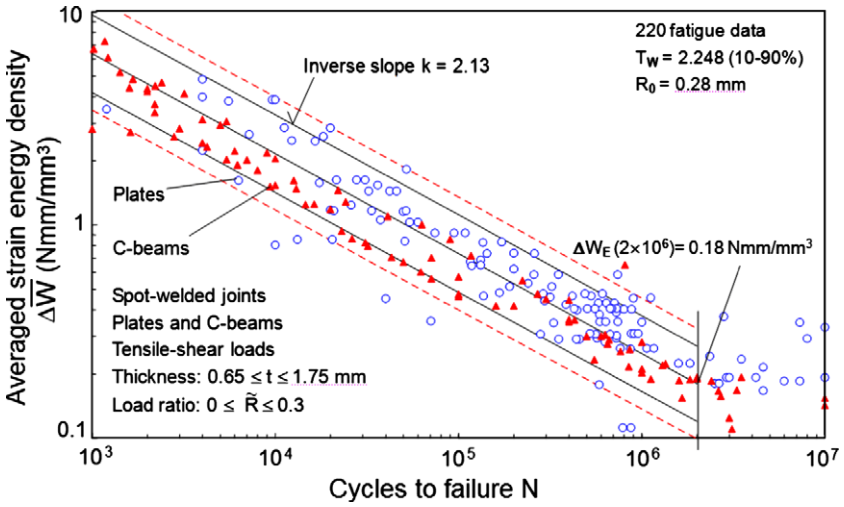

Fig. 10. Synthesis of data from spot-welded joints under tension and shear loading. The thickness t ranges from 0.65 to 1.75 mm. SED values have been determined by means of three-dimensional models. The control radius of the volume and its depth are equal to 0.28 mm.

0.070 mm (ultimate tensile strength σ_t = 72.57 MPa, fracture toughness $K_{IC} = 37.1$ MPa mm$^{0.5}$, the Young's modulus E = 3230 MPa and the Poisson's ratio ν = 0.30). In the presence of tensile loads, the geometries assured a strong variability of the mode I and mode II notch stress intensity factors. However all the specimens were subjected to prevalent mode I. A new test configuration for mixed-mode fracture was proposed in Ref. [80] and a complete set of experimental data from diagonally loaded square cracked plate specimens made of PMMA ranging from pure mode I to pure mode II was provided.

New interesting data from pointed V-notches samples made of PMMA and tested at low temperature under prevalent mode II loading are available in Refs [61,81]. The problem of brittle failure from *blunted notches* loaded under *mixed mode* is more complex than in mode I loading and experimental data, particularly for notches with a non-negligible radius, is scarce. The experimental programme has been performed with V-notched specimens, varying the notch inclination, the notch angle and the boundary conditions to obtain different mode (I + II) mixity. The new research is focused on sharp notches and the notch root radius, R, is always less than 0.1 mm, ranging between 20 and 72 μm. To achieve different mixed-mode loading and to analyse the field of prevalent mode II, two types of V-notched specimens were studied; beams with *vertical* notches, with notch angles, α: 30°, 60° and 90°, and beams with *tilted* notches at 45°, with notch angles 30° and 60° and 90°. Samples are loaded by using a three point bending configuration. The position of the loading point is modified such as the span length to vary the mode I contribution respect to mode II contribution. Dealing with the new results summarised in [61], the ratio $\chi = W_1/W_{tot}$ which gives the mixity degree in terms of local SED has been analysed (see Fig. 11). The mean value of the ratio $\sqrt{\overline{W}/W_c}$ to which the critical loads are linked, is found to be about equal to 1.0 but values greater than 1.1 characterize specimens with $\chi \approx 1.0$ (dominant mode I), $\chi = 0.27$ (dominant mode II) and $0.52 \leqslant \chi \leqslant 0.64$ (mode II comparable with mode I) independently of the mode mixity being this effect tied to the intrinsic scatter of the experimental data.

The final synthesis has been carried out by normalising the local SED to the critical SED values (as determined from unnotched, plain specimens) and plotting this non-dimensional parameter as a function of the R/R_0 ratio. A scatterband is obtained whose mean value does not depend on R/R_0, whereas the ratio between the upper and the lower limits are found to be about equal to 1.3/

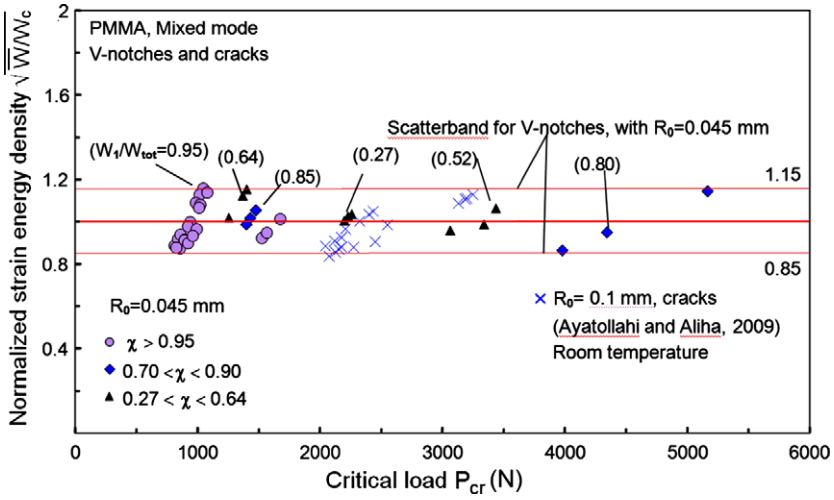

Fig. 11. Synthesis of all experimental data from pointed V-notched plates based on two different values of the control volume radius; comparison with recent results from cracked plates tested at room temperature [61].

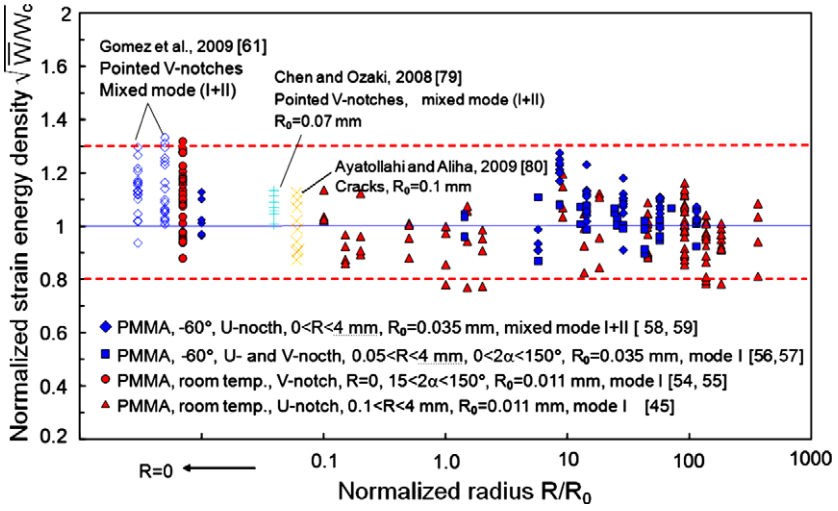

Fig. 12. Static failure data in terms of normalised strain energy density.

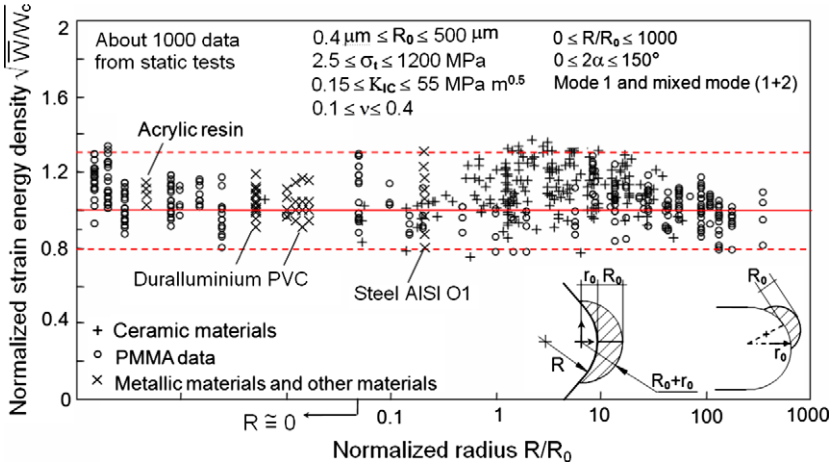

Fig. 13. Synthesis of data taken from the literature. Different materials are summarised, among the others AISI O1 and duralluminium.

0.8 = 1.6 (Fig. 12). The strong variability of the non-dimensional radius R/R_0 (notch root radius to control volume radius ratio, ranging here from about zero to about 500) makes stringent the check of the approach based on the local SED. The complete scatterband presented here for the first time (Fig. 13) has been obtained by updating the database containing failure data from 20 different ceramics, 4 PVC foams and some metallic materials [60] with the new results reported in Refs [61,79,80].

4. Conclusions

For many years the Strain Energy Density (SED) has been used to formulate failure criteria for materials exhibiting both ductile and brittle behaviour. SED is the most fundamental quantity in Mechanics being all physical quantities expressible in terms of it. From pico- to macroscopic scale the energy absorption and dissipation can explain the most complex phenomena tied to fracture initiation and propagation.

Keeping in mind that the design rules valid for large bodies (i.e. high volume to surface ratio) can not be directly translated and applied to small bodies where local inhomogeneities play a fundamental role for the material damage initiation and propagation and being also aware of the recent contributions and efforts to develop a multiscaling and segmentation scheme able to capture the complex phenomena that happen at every level from pico to macro, the main purpose of the paper is to present a review of the approach based on the mean value of the local strain energy density.

Dealing with static loading the approach is applied here to different materials and geometries both, under mode I and mixed-mode (I + II) loading. About one thousand experimental data, taken from the recent literature, are involved in the synthesis. They were from U- and V-notched specimens made of very different materials. A scatter band is proposed by using as a synthesis parameter the value of the local energy averaged over control volume (of radius R_0), normalised by the critical energy of the material. Such a normalised energy is plotted as a function of the notch radius to critical radius ratio, R/R_0.

The Strain Energy Density (SED) in a circular sector of radius R_0 located at the crack initiation sites has successfully been used to summarise also about nine hundred data from fatigue failures of welded joints.

Under the hypothesis that all material inhomogeneities can be averaged, that ceases to be valid at pico- and micro-levels but at the same time is the basis of the volume-based theories applied

to structural components, the Strain Energy Density Approach is shown to be a powerful tool both for static and fatigue strength assessment of notched and welded structures.

References

[1] X.S. Tang, G.C. Sih, Weak strong singularities reflecting multiscale damage: micro-boundary conditions for free–free, fixed–fixed and free–fixed constraints, Theoretical and Applied Fracture Mechanics 43 (2005) 5–62.
[2] G.C. Sih, X.S. Tang, Scaling of volume energy density function reflecting damage by singularities at macro-, meso- and microscopic level, Theoretical and Applied Fracture Mechanics 43 (2005) 211–231.
[3] G.C. Sih, Multiscaling in Molecular and Continuum Mechanics: Interaction of Time and Size from Macro to Nano, Springer, Dordrecht, 2007.
[4] G.C. Sih, Crack tip mechanics based on progressive damage of arrow: hierarchy of singularities and multiscale segments, Theoretical and Applied Fracture Mechanics 51 (2009) 11–32.
[5] G.C. Sih, Ideomechanics of transitory and dissipative systems associated with length, velocity, mass and energy, Theoretical and Applied Fracture Mechanics 51 (2009) 149–160.
[6] G.C. Sih, Energy absorption and dissipation associated with mass activation and deactivation for open systems, Theoretical and Applied Fracture Mechanics 52 (2009) 63–71.
[7] P. Lazzarin, R. Zambardi, A finite-volume-energy based approach to predict the static and fatigue behaviour of components with sharp V-shaped notches, International Journal of Fracture 112 (2001) 275–298.
[8] P. Lazzarin, T. Lassen, P. Livieri, A notch stress intensity approach applied to fatigue life predictions of welded joints with different local toe geometry, Fatigue and Fracture of Engineering Materials and Structures 26 (2003) 49–58.
[9] P. Lazzarin, C.M. Sonsino, R. Zambardi, A notch stress intensity approach to assess the multiaxial fatigue strength of welded tube-to flange joints subjected to combined loadings, Fatigue and Fracture of Engineering Materials and Structures 27 (2004) 127–140.
[10] P. Livieri, P. Lazzarin, Fatigue strength of steel and aluminium welded joints based on generalised stress intensity factors and local strain energy values, International Journal of Fracture 133 (2005) 247–278.
[11] P. Lazzarin, F. Berto, Berto Some expressions for the strain energy in a finite volume surrounding the root of blunt V-notches, International Journal of Fracture 135 (2005) 161–185.
[12] P. Lazzarin, F. Berto, From Neuber's elementary volume to Kitagawa and Atzori's diagrams: an interpretation based on local energy, International Journal of Fracture 135 (2005) L33–L38.
[13] P. Lazzarin, P. Livieri, F. Berto, M. Zappalorto, Local strain energy density and fatigue strength of welded joints under uniaxial and multiaxial loading, Engineering Fracture Mechanics 75 (2008) 1875–1889.
[14] P. Lazzarin, F. Berto, Control volumes and strain energy density under small and large scale yielding due to tensile and torsion loading, Fatigue and Fracture of Engineering Materials and Structures 31 (2008) 95–107.
[15] H. Neuber, Kerbspannungslehre, second ed., Springer-Verlag, Berlin, 1958.
[16] H. Neuber, Über die Berücksichtigung der Spannungskonzentration bei Festigkeitsberechnungen, Konstruktion 20 (1968) 245–251.
[17] H. Neuber, Kerbspannungslehre, third ed., Springer-Verlag, Berlin, 1985.
[18] F.A. McClintock, Ductile fracture instability in shear, Journal of Applied Mechanics 25 (1958) 582–588.
[19] R.O. Ritchie, J. Knott, J.R. Rice, On the relation between critical tensile stress in fracture toughness in mild steel, Journal of the Mechanics and Physics of Solids 21 (1973) 395–410.
[20] Z. Knésl, A criterion of V-notch stability, International Journal of Fracture 48 (1991) R79–R83.
[21] A. Seweryn, Brittle fracture criterion for structures with sharp notches, Engineering Fracture Mechanics 47 (1994) 673–681.
[22] V.V. Novozhilov, On necessary and sufficient criterion of brittle fracture, Prikladnaja Matematika i Mechanika 33 (1969) 212–222.
[23] A. Seweryn, Z. Mróz, A non-local stress failure condition for structural elements under multiaxial loading, Engineering Fracture Mechanics 51 (1995) 955–973.
[24] A. Seweryn, S. Poskrobko, Z. Mróz, Brittle fracture in plane elements with sharp notches under mixed-mode loading, Journal of Engineering Mechanics 123 (1997) 535–543.
[25] S.D. Sheppard, Field effects in fatigue crack initiation: long life fatigue strength, Transactions of the ASME. Journal of Mechanical Design 113 (1991) 188–194.
[26] E. Beltrami, Sulle condizioni di resistenza dei corpi elastici, Rend. R. Ist. Lombardo di Scienze, Lettere e Arti 18 (1885) 704 (in Italian).
[27] G.C. Sih, A special theory of crack propagation: methods of analysis and solutions of crack problems, in: G.C. Sih (Ed.), Mechanics of Fracture, Noordhoff International Publishing, Leyden, 1973, pp. 21–45.
[28] G.C. Sih, Strain–energy–density factor applied to mixed mode crack problems, International Journal of Fracture 10 (1974) 305–321.
[29] G.C. Sih, Surface layer energy and strain energy density for a blunted crack or notch, in: G.C. Sih, H.C. van Elst, D. Broek (Eds.), Prospect of Fracture Mechanics, Noordhoff International Publishing, Leyden, 1974, pp. 85–102.
[30] G.C. Sih, Mechanics of Fracture Initiation and Propagation: Surface and Volume Energy Density Applied as Failure Criterion, Kluwer Academic Publisher, Dordrecht, 1991.
[31] G.C. Sih, J.W. Ho, Sharp notch fracture strength characterized by critical energy density, Theoretical Applied Fracture Mechanics 16 (1991) 179–214.
[32] G.C. Sih, E. Czoboly, L.F. Gillemot (Eds.), Absorbed Specific Energy and Strain Energy Density Criterion, Proceedings of an International Symposium on Absorbed Specific Energy and Strain Energy Density Criterion, Budapest, September 1980. In memory of the late Professor L.ászló Gillemot, Martinus Nijhoff Publishers, The Netherlands, 1982.
[33] L.F. Gillemot, Brittle fracture of welded materials, in: Commonwealth Welding Conference, vol. C.7, 1965, pp. 353–358.
[34] L.F. Gillemot, Criterion of crack initiation and spreading, Engineering Fracture Mechanics 8 (1976) 239–253.
[35] L.F. Gillemot, E. Czoboly, I. Havas, Fracture mechanics applications of absorbed specific fracture energy: notch and unnotched specimens, Theoretical and Applied Fracture Mechanics 4 (1985) 39–45.
[36] E.E. Gdoutos, Fracture Mechanics Criteria and Applications, Kluwer Academic Publishers, Dodrecht/Boston/London, 1990.
[37] G. Glinka, K. Molski, A method of elastic–plastic stress and strain calculation at a notch root, Material Science Engineering 50 (1981) 93–100.
[38] G. Glinka, Energy density approach to calculation of inelastic strain–stress near notches and cracks, Engineering Fracture Mechanics 22 (1985) 485–508.
[39] F. Ellyin, Fatigue Damage, Crack Growth and Life Prediction, Chapman & Hall, London, 1997.
[40] F. Ellyin, D. Kujawski, Generalization of notch analysis and its extension to cyclic loading, Engineering Fracture Mechanics 32 (1989) 819–826.
[41] Z. Yosibash, Ar Bussiba, I. Gilad, Failure criteria for brittle elastic materials, International Journal of Fracture 125 (2004) 307–333.
[42] M.E. Kipp, G.C. Sih, The strain energy density failure criterion applied to notched elastic solids, International Journal of Solids and Structures 11 (1975) 153–173.
[43] A. Carpinteri, Stress singularity and generalised fracture toughness at the vertex of re-entrant corners, Engineering Fracture Mechanics 26 (1987) 143–155.
[44] L.S. Nui, C. Chehimi, G. Pluvinage, Stress field near a large blunted tip V-Notch and application of the concept of the critical notch stress intensity factor (NSIF) to the fracture toughness of very brittle materials, Engineering Fracture Mechanics 49 (1994) 325–335.
[45] F.J. Gómez, M. Elices, A. Valiente, Cracking in PMMA containing U-shaped notches, Fatigue and Fracture of Engineering Materials and Structures 23 (2000) 795–803.
[46] B. Atzori, P. Lazzarin, Notch sensitivity and defect sensitivity: two sides of the same medal, International Journal of Fracture 107 (2001) L3–L8.
[47] M. Strandberg, Fracture at V-notches with contained plasticity, Engineering Fracture Mechanics 69 (2002) 403–415.
[48] B. Atzori, P. Lazzarin, G. Meneghetti, Fracture mechanics and notch sensitivity, Fatigue and Fracture of Engineering Materials and Structures 26 (2003) 257–267.
[49] G.A. Gogotsi, Fracture toughness of ceramics and ceramic composites, Ceramics International 7 (2003) 777–884.
[50] D. Leguillon, Z. Yosibash, Crack onset at a V-notch. Influence of the notch tip radius, International Journal of Fracture 122 (2003) 1–21.
[51] D. Dini, D. Hills, Asymptotic characterisation of nearly-sharp notch root stress field, International Journal of Fracture 130 (2004) 651–666.
[52] Z. Yosibash, E. Priel, D. Leguillon, A failure criterion for brittle elastic materials under mixed-mode loading, International Journal of Fracture 141 (2006) 291–312.
[53] D. Leguillon, D. Quesada, C. Putot, E. Martin, Prediction of crack initiation at blunt notches and cavities – size effects, Engineering Fracture Mechanics 74 (2007) 2420–2436.
[54] F.J. Gómez, M. Elices, Fracture of components with V-shaped notches, Engineering Fracture Mechanics 70 (2003) 1913–1927.
[55] F.J. Gómez, M. Elices, A fracture criterion for sharp V-notched samples, International Journal of Fracture 123 (2003) 163–175.
[56] F.J. Gómez, M. Elices, A fracture criterion for blunted V-notched samples, International Journal of Fracture 127 (2004) 239–264.
[57] F.J. Gómez, M. Elices, J. Planas, The cohesive crack concept: application to PMMA at −60 °C, Engineering Fracture Mechanics 72 (2005) 1268–1285.
[58] F.J. Gómez, M. Elices, F. Berto, P. Lazzarin, Local strain energy to asses the static failure of U-notches in plates under mixed mode loading, International Journal of Fracture 145 (2007) 29–45.
[59] F. Berto, P. Lazzarin, F.J. Gomez, M. Elices, Fracture assessment of U-notches under mixed mode loading: two procedures based on the 'equivalent local mode I' concept, International Journal of Fracture 148 (2007) 415–433.
[60] P. Lazzarin, F. Berto, M. Elices, J. Gómez, Brittle failures from U- and V-notches in mode I and mixed, I+II, mode. A synthesis based on the strain energy density averaged on finite size volumes, Fatigue and Fracture of Engineering Materials and Structures 32 (2009) 671–684.
[61] F.J. Gómez, M. Elices, F. Berto, P. Lazzarin, Fracture of v-notched specimens under mixed mode (I + II) loading in brittle materials, International Journal of Fracture 159 (2009) 121–135.
[62] F. Erdogan, C.G. Sih, On the crack extension in plates under plane loading and transverse shear, Journal of Basic Engineering (1963) 519–525.
[63] F. Schleicher, Der Spannungszustand an der Fliessgrenze (Plastizitätsbedingung), Zeitschrift für angewandte Mathematik und Mechanik 6 (3) (1926) 199–216.
[64] S. Filippi, P. Lazzarin, R. Tovo, Developments of some explicit formulas useful to describe elastic stress fields ahead of notches in plates, International Journal of Solids and Structures 39 (2002) 4543–4565.
[65] M.L. Williams, Stress singularities resulting from various boundary conditions in angular corners on plates in tension, Journal of Applied Mechanics 19 (1952) 526–528.

[66] M. Creager, P.C. Paris, Elastic field equations for blunt cracks with reference to stress corrosion cracking, International Journal of Fracture Mechanics 3 (1967) 247–252.
[67] R. Gross, A. Mendelson, Plane elastostatic analysis of V-notched plates, International Journal of Fracture Mechanics 8 (1972) 267–276.
[68] P. Lazzarin, S. Filippi, A generalised stress intensity factor to be applied to rounded V-shaped notches, International Journal of Solids and Structures 43 (2006) 2461–2478.
[69] P. Lazzarin, F. Berto, F.J. Gómez, M. Zappalorto, Some advantages derived from the use of the strain energy density over a control volume in fatigue strength assessments of welded joints, International Journal of Fatigue 30 (2008) 1345–1357.
[70] P. Lazzarin, F. Berto, M. Zappalorto, Mean values of the strain energy density from coarse meshes: theoretical bases of a method suitable for rapid calculations of notch stress intensity factors and fatigue strength of welded joints. International Journal of Fatigue, submitted for publication.
[71] P. Lazzarin, F. Berto, D. Radaj, Stress intensity factors of welded lap joints: a comparison between pointed slit based and keyhole notch based models, with extensions to strain energy density and J-integral, Fatigue and Fracture of Engineering Materials and Structures 32 (2009) 713–735.
[72] A. Kotousov, C.H. Wang, Three dimensional stress constraint in an elastic plate with a notch, International Journal of Solids and Structures 39 (2002) 4311–4326.
[73] F. Berto, P. Lazzarin, C.H. Wang, Three-dimensional linear elastic distributions of stress and strain energy density ahead of V-shaped notches in plates of arbitrary thickness, International Journal of Fracture 127 (2004) 265–282.
[74] A. Kotousov, T.L. Lew, Stress singularities resulting from various boundary conditions in angular corners of plates of arbitrary thickness in extension, International Journal of Solids and Structures 43 (2005) 5100–5109.
[75] A. Kotousov, Fracture in plates of finite thickness, International Journal of Solids and Structures 44 (2007) 8259–8273.
[76] S. Harding, A. Kotousov, P. Lazzarin, F. Berto, Transverse singular effects in V-shaped notches stressed in mode II, International Journal of Fracture (2009).
[77] B. Atzori, V. Dattoma, A comparison of the fatigue behaviour of welded joints in steels and in aluminium alloys, IIW Doc XXXIII (1983) 1089–1983.
[78] D. Radaj, Design and Analysis of Fatigue Resistant Welded Structures, Abington Publishing, Cambridge, 1990.
[79] D.H. Chen, S. Ozaki, Investigation of failure criteria for a sharp notch, International Journal of Fracture 152 (2008) 63–74.
[80] M.R. Ayatollahi, M.R.M. Aliha, Analysis of a new specimen for mixed mode fracture tests on brittle materials, Engineering Fracture Mechanics 76 (2009) 1563–1573.
[81] F. Berto, P. Lazzarin, F.J. Gomez, M. Elices, Brittle Failure and Crack Initiation Angle in Plates Weakened by V- and U-Notches Under Mixed Mode (I + II) Loading. Crack Paths CP 2009, 23–25 September 2009, Vicenza, Italy.